Angewandte Chemie
Eine Zeitschrift der Gesellschaft Deutscher Chemiker

Supporting Information

Antivitamin B_{12} Inhibition of the Human B_{12}-Processing Enzyme CblC: Crystal Structure of an Inactive Ternary Complex with Glutathione as the Cosubstrate

Markus Ruetz, Aranganathan Shanmuganathan, Carmen Gherasim, Agnes Karasik, Robert Salchner, Christoph Kieninger, Klaus Wurst, Ruma Banerjee, Markos Koutmos,* and Bernhard Kräutler**

ange_201701583_sm_miscellaneous_information.pdf

General.

Materials. Aquocobalamin chloride *Roussel UCLAF;* water was purified using Epure, Barnstead Co; N-iodomorpholine was prepared as described [1], 2,4-diflourophenylethyne, *Sigma-Aldrich* (*97%*), formic acid *purum*, triethylamine, *puriss*, *Fluka*, copper(I)iodide, Merck, acetonitrile (MeCN) and methanol (MeOH) HPLC-grade, *BDH prolabo*, dichloromethane ($MeCl_2$), Acros, was distilled prior to use, tetrahydrofuran (THF) purum, Merck; CD_3OD (99,80%D) Eurisotop; LiChroprep RP-18 (25-40µm), *Merck*, Aluminum oxide activated neutral, *Sigma Aldrich*, dimethylsulfoxide (DMSO), distilled. Tris(2-carboxyethyl)phosphine (TCEP), *GoldBio*, 4-(2-hydroxyethyl)-1-piperazineethanesulfonic acid (HEPES), *Fisher Scientific*, potassium chloride (KCl), *Fisher Scientific*, glycerol, *Fisher Scientific*, glacial acetic acid and acetonitrile (both HPLC grade), *Fisher Scientific*. Glutathione (GSH), *Sigma Aldrich*.

Spectroscopy for characterization of iodo-2-(2,4-difluorophenyl)eth-1-yne and of 2-(2,4-difluorophenyl)ethynyl-cobalamin (**3**, F2PhEtyCbl). *UV/Vis*: Agilent Technologies Cary 60; λ_{max} (log ε) in nm. *CD*: Jasco J715; λ_{max} or λ_{min} (Δ ε) in nm. *FT-IR*: Mattson 300 Galaxy Series; cm^{-1}. *^{1}H and ^{13}C-NMR:* Bruker AM 300 (for 1-iodoalkynes), 500 MHz Varian Unity Inova (for cobalamins), equipped with 5 mm triple-resonance probe with z-gradients; δ(HDO) = 4.77 ppm; δ(CD_3OD) = 3.31 ppm, δ(DMSO-d6) = 2.50 ppm; HSQC: 2k x 512 complex data points. SW2: 11 ppm centred on residual water signal, SW1: -10-200 ppm. 64 scans per increment. HMBC: 2k x 512 data points (real). SW2: 11 ppm centred on residual water signal, SW1: -10-200 ppm. 64 scans per increment. ROESY: 2k x 512 complex data points, 32 scans per t1 increment, mixing time 250 ms. *MALDI-MS*: Bruker Ultraflex MALDI-TOF, positive-ion mode, matrix: 2,5-dihydroxybencoic acid.

Synthetic Procedures

Synthesis of 1-iodo-2-(2,4-difluorophenyl)eth-1-yne (procedure modified from [1]).

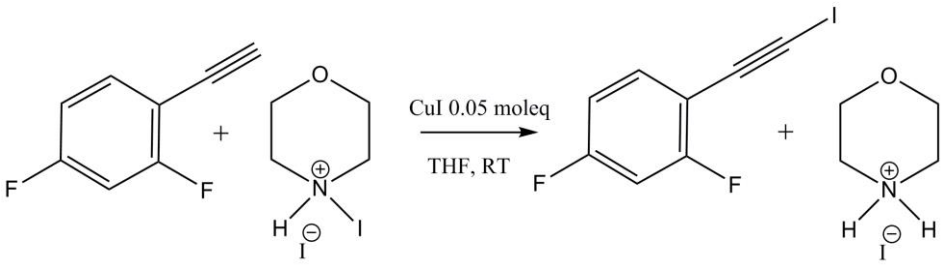

In a 5 ml round bottom flask, 301.3 mg 4-iodomorpholin-4-ium iodide (0.88 mmol), 110.5 mg 2,4-difluorophenylethyne (0,80 mmol) and 7.6 mg copper(I)iodide (0.040 mmol) were mixed with 2 ml of distilled THF at room temperature. The mixture was stirred for one hour (white precipitate formed). The reaction mixture was then poured on a pad of activated neutral aluminum oxide (3.6 g). The material was washed four times with CH_2Cl_2 (2 ml each). The filtrates were collected and dried using a rotary evaporator. The remaining yellow oil was dropped into 10 ml of n-hexane to precipitate residual morpholine. The brown precipitate was filtered off using a Büchner funnel. The filtrate was dried on a rotary evaporator giving 177.9 mg 1-iodo-2-(2,4-difluorophenyl)ethyne (0.674 mmol, 84.3 % yield) as yellowish crystals with the following spectral data:

^{1}H-NMR: (300 MHz, $CDCl_3$, 298 K): δ [ppm] = 7.37-7.45 (*m*, 1 H); 6.80-6.87 (*m*, 2 H)

Synthesis of 2-(2,4-difluorophenyl)ethynyl-cobalamin (**3, F2PhEtyCbl**), adapted from [2]**)**

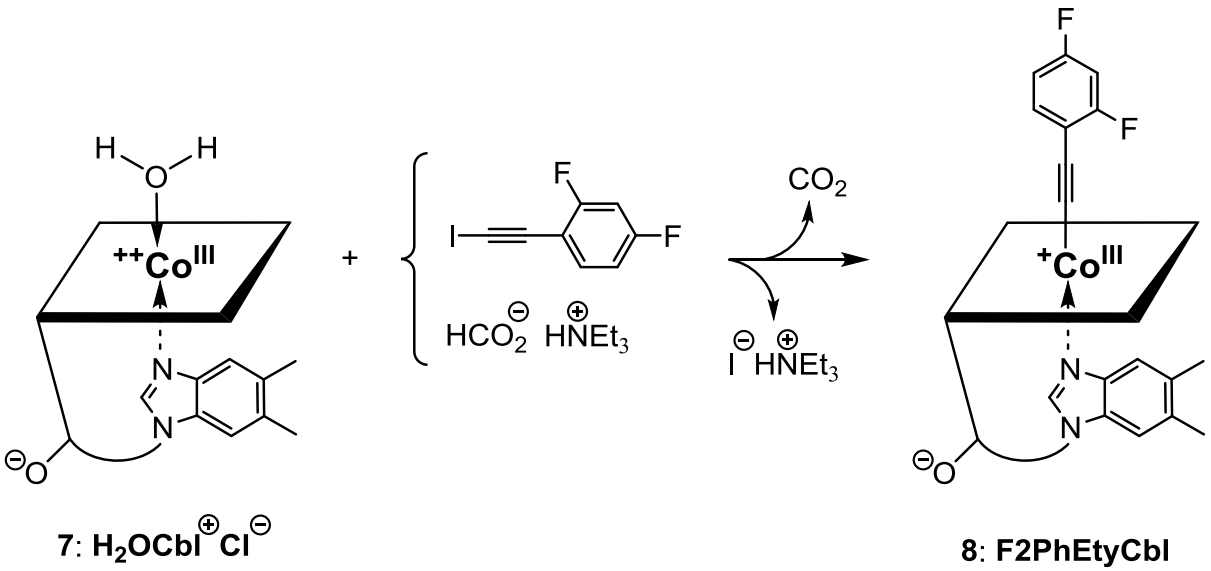

7: $H_2OCbl^{\oplus}Cl^{\ominus}$ **8**: **F2PhEtyCbl**

In a 5 ml round bottom flask, 100.0 mg of aquocobalamin chloride (H_2OCbl) (72.3 µmol) were dissolved in 2.5 ml of MeOH and the mixture was degassed with argon for 10 min. To this solution 50 µl formic acid (1.3 mmol) and 187 µl triethylamine (1.3 mmol) were added under argon and the solution was stirred for 30 min at RT. To the now brown solution a 58.4 mg 1-iodo-2-(2,4-difluorophenyl)eth-1-yne (222.0 µmol), dissolved in 25 µl CH_2Cl_2, were added under argon and the mixture was stirred for another hour. The reaction mixture was poured in 15 ml of ethyl acetate to precipitate the raw product. The mother liquor was removed and the red precipitate was dried under high vacuum for 2 hours. The raw product was purified by RP-18 column chromatography using MeOH/H_2O, solvent system (10-70% MeOH, in 10% steps). At first, H_2OCbl eluted at 30 % MeOH followed, at 50 % MeOH, by the red fraction of the product **3**. The product fraction was collected and the solvents were evaporated on rotary evaporator at room temperature. Raw red corrin was dissolved in water (0.5 ml) and crystallized after addition of 5 ml of acetone. The crystals of **3** were first washed with (1:9) mixture of water: acetone, then with acetone. The sample of **3** was dried under high vacuum overnight, to give 61.7 mg (42.1 µmol, 58.2% yield) of red crystalline solid, which was characterized as follows: **TLC:** RP-18, MeOH/H_2O (3/7): R_f = 0.78. **UV/Vis:** (c = 5.0 x 10^{-5} M, 50 mM phosphate buffer pH7): λ_{max} (log ε) = 550 (3.84), 527 (3.80), 403 (3.67), 364 (4.10), 354 sh (4.09), 274 sh (4.43) 256 (454) nm. **CD:** (c = 7.92 x 10^{-5} M, H_2O): λ_{max}, λ_{min}; 557 (–3.4), 498 (3.6), 452 (-3.0), 394 (3.8), 352 (3.2), 316 (-3.3), 281 (–3.4), 249 (-4.3) nm (mol^{-1} cm^3 cm^{-1}); λ_0: 580,525,380, 270, 251, 246, 220 nm (see Figure S1). **IR**: (KBr): υ = 3386 (vs), 2968 (m), 2130 (w) 1666 (vs) 1573 (s) 1497 (vs) 1402 (s), 1351 (m), 1215 (s), 1142 (s), 1091(s), 998 (m) 996 (m) 850 (m), 812 (m),597 (m); cm^{-1}(see Figure S2). **^{1}H-NMR:** (500 MHz, 298 K, CD_3OD, c = 7.7 mM) δ = 0.51 (*s*, 3H, H_3C-1A); 1.13 (*s*, 3H, H_3C-12B); 1.29 (*m*, 1H, H_aC-81); 1.27 (*d*, 3H, J = 6.2 Hz, H_3C-177); 1.30 (*s*, 3H, H_3C-17B); 1.35 (*m*, 1H, H_aC-82); 1.36 (*s*, 3H, H_3C-2A); 1.48 (*s*, 3H, H_3C-12A); 1.75 (*m*, 1H, H_bC-82); 1.84 (*m*, 1H, H_aC-172); 1.86 (*s*, 3H, H_3C-7A); 1.91 (*m*, 1H, H_aC-131); 1.94 (*m*, 2H, H_2C-31); 2.02 (*m*, 1H, H_bC-81); 2.05 (*m*, 1H, H_aC-71); 2.07 (*m*, 1H, H_bC-131); 2.23 (*m*, 1H, H_aC-171); 2.29 (*s*, 3H, H_3C-10N); 2.30 (*s*, 3H, H_3C-11N); 2.32 (*m*, 1H, H_aC-21); 2.43 (*m*, 1H, H_bC-71); 2.45 (*m*, 2H, H_2C-32); 2.53 (*m*, 1H, H_bC-21); 2.54 (*m*, 2H, H_2C-132); 2.55 (*m*, 1H, H_aC181); 2.57 (*s*, 3H, H_3C-151); 2.59 (*m*, 1H, H_bC-171); 2.61 (*m*, 1H, H_bC-181); 2.63 (*s*, 3H, H_3C-51); 2.63 (*m*, 1H, H_bC-172); 2.85 (*m*, 1H, HC-18); 2.88 (*m*, 1H, H_aC-175); 3.24 (*d*, 1H, J = 10.6, HC-13); 3.60 (*m*, 1H, HC-8); 3.69 (*d*, 1H, J = 14.9 Hz, H_bC-175); 3.78 (*dxd*; 1H, J =12.4; 4.5 Hz; H_aC-5R); 3.94 (*dxd*; 1H, J = 12.4, 3.4 Hz H_bC-5bR); 4.13 (*m*, 1H, HC-4R); 4.22 (*t*, 1H, J = 7.0, 3.6

Hz, HC-2R); 4.35 (*m*, 1H, HC-176); 4.45 (*d*, 1H, J = 11.5 Hz, HC-19); 4.61 (*d*, 1H, J = 8.9 Hz, HC-3); 4.69 (*m*, 1H, HC-3R); 6.01 (*s*, 1H, HC-10); 6.28 (*d*, 1H, J = 3.2 Hz HC-1R); 6.64 (*s*, 1H, HC-4N); 6.70 (*dxt*, 1H, J = 2.3, 9.4 Hz HC-7L), 6.76 (*dxt*, 1H, J = 2.5, 8.8 Hz, HC-5L); 6.84 (*s*, 1H, HC-8L) 7.22 (*s*, 1H, HC-2N); 7.24 (*s*, 1H, HC-7N) (see Figures S3 and S4 - for atom numbering). **^{13}C-NMR:** (125 MHz, 298 K, CD_3OD, c = 7.7 mM) δ = 16.34 (C51); 16.43 (C151); 17.58 (C17B); 17.62 (C2A); 20.20 (C7A); 20.44 (C12A); 20.53 (C177); 20.76 (C11N); 20.88 (C1A); 20.89 (C10N); 27.55 (C31); 27.62 (C81); 29.79 (C131); 32.10 (C12B); 33.02 (C171); 33.38 (C82); 33.68 (C172); 35.66 (C132); 36.68 (C32); 40.03 (C18); 43.40 (C21); 44.10 (C181), 44.17 (C71); 46.86 (C175); 48.44 (C2); 49.39 (C12), 52.38 (C7), 55.29 (C13); 57.02 (C8); 57.13 (C3), 60.08 (C17); 62.87 (C5R); 70.92 (C2R); 73.76 (C176); 75.71 (C3R); 75.97 (C19); 83.64 (C4R); 86.39 (C1); 87.99 (C1R); 93.56 (C2L); 95.48 (C10); 104.48 (C5L); 104.97 (C15); 108.54 (C5); 112.1 (C3L); 112.24 (C7L); 112.24 (C7N); 118.73 (C4N); 131.82 (C9N); 133.19 (C6N); 134.87 (C8L); 135.18 (C5N); 138.82 (C8N); 143.97 (C2N); 163.30 (C6L); 165.34 (C4L); 165.86 (C6); 166.44 (C149); 173:98 (C9); 174.58 (C173); 175.24 (C72); 175.84 (C182); 176.24 (C11); 176.45 (C22); 177.03 (C83); 177.82 C(33); 178.28 (C16); 179.65 (C4). **MS** (MALDI-TOF): m/z (%) = 1487.5 (13, $[M+Na]^+$), 1466.4 (20, $[M+H]^+$), 1367.4 (47, [M-(2,4-difluorophenyl-ethyne)+K]$^+$), 1351.4 [M-(2,4-difluorophenyl-ethyne)+Na]$^+$), 1329.7 (100, [M-(2,4-difluorophenyl-ethyne)]$^+$), 1201.9 (43, [M-(2,4-difluorophenyl-ethyne)-nucleotide base]$^+$), 1184.30 (13, [M-L-B] $^+$); 1067.4 (16, [M-(2,4-difluorophenylethyne)-$C_{14}H_{17}N_2O_3]^+$, 971.3 (30, [M-(2,4-difluorophenyl-ethyne-$C_{14}H_{18}N_2O_7P]^+$.

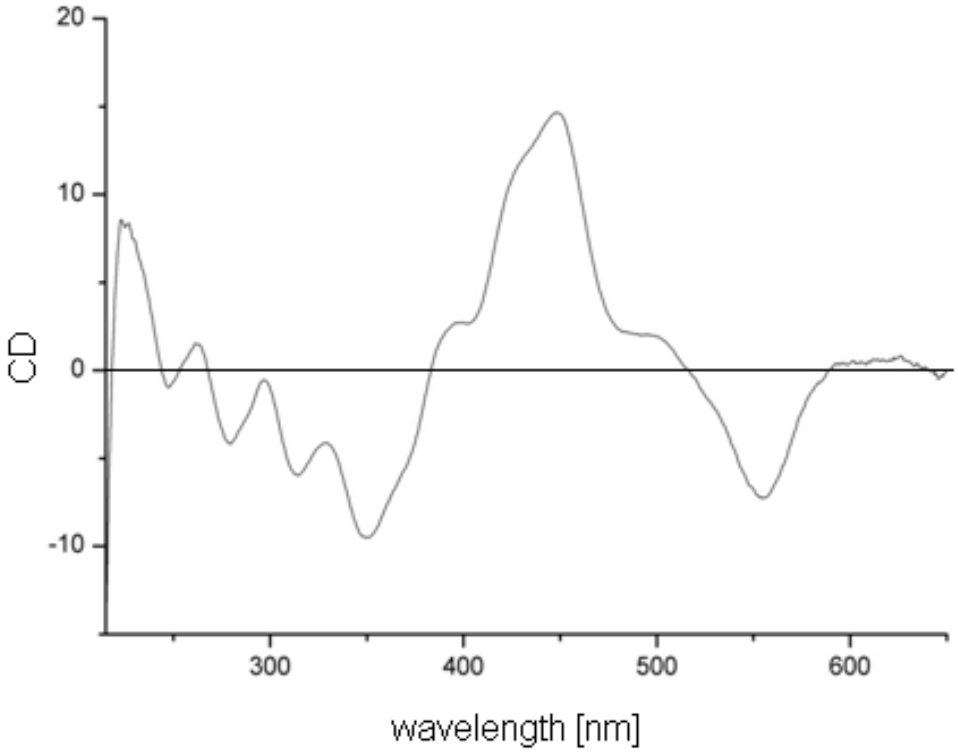

Figure S1: CD spectrum of F2PhEtyCbl (**3**) in H_2O

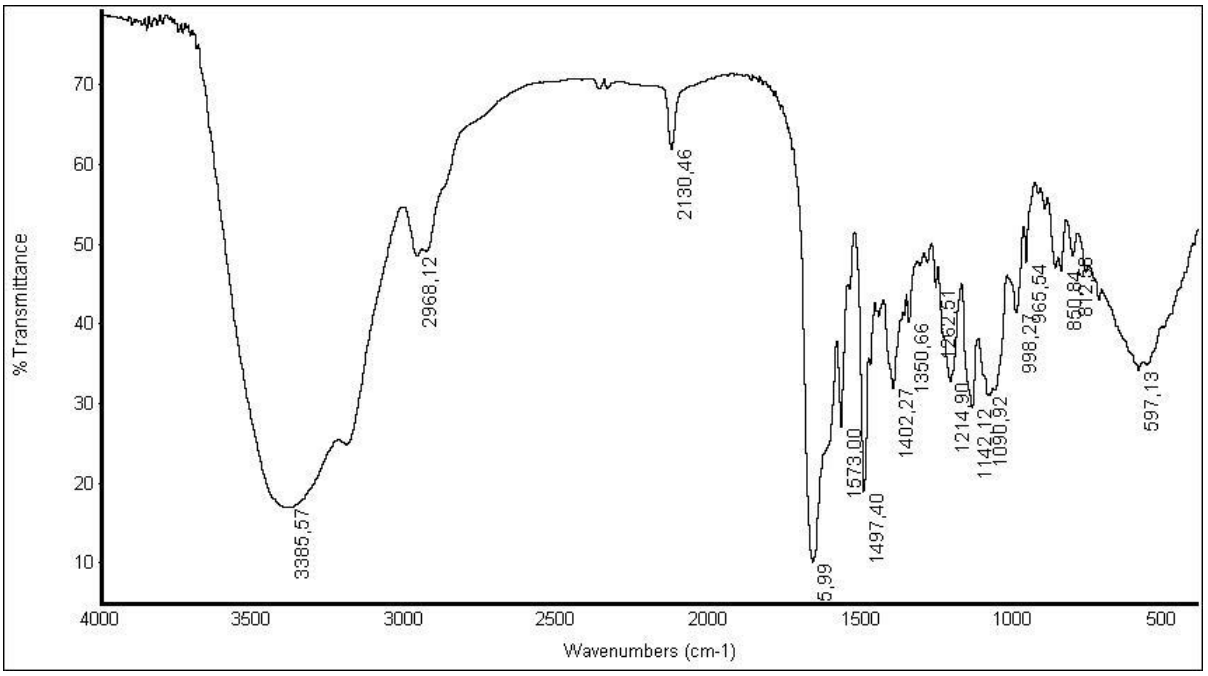

Figure S2: IR spectrum of F2PhEtyCbl (**3**) in KBr

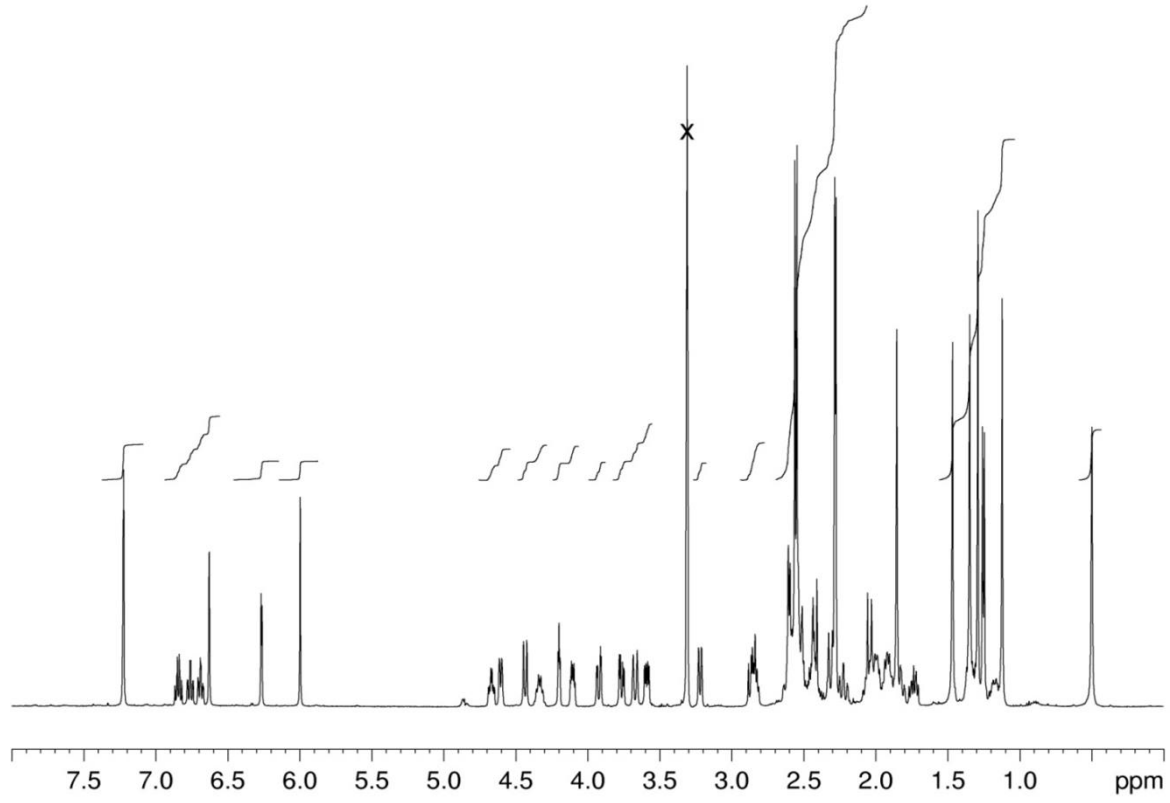

Figure S3: 500 MHz ^{1}H-NMR-spectrum of F2PhEtyCbl (**3**) in CD_3OD (X = residual solvent signal, small signal near 4.8 ppm corresponds to residual HDO).

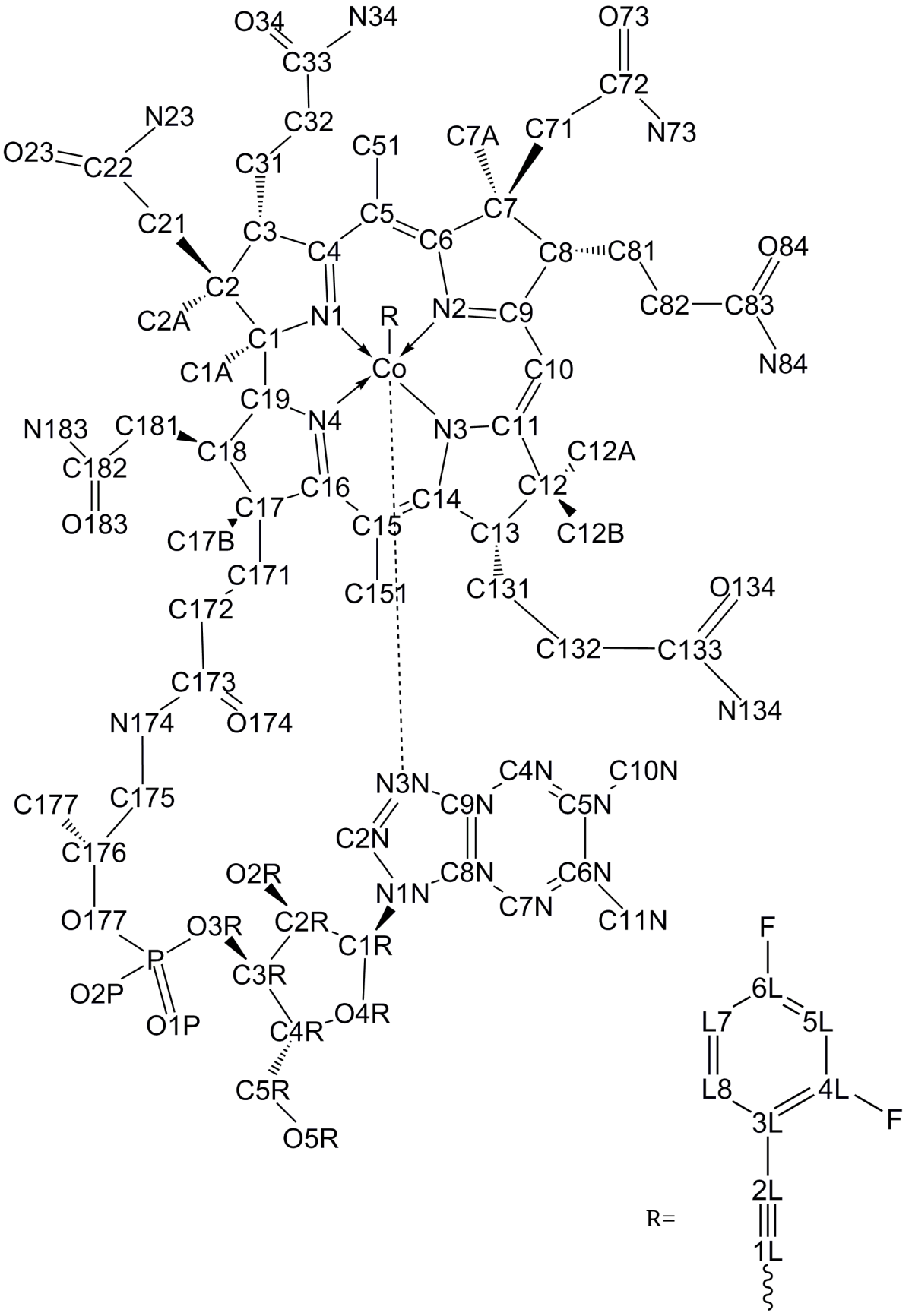

Figure S4. Atom numbering used for NMR and X-ray crystal analysis of F2PhEtyCbl (**3**).

Crystal structure of Co_β-2-(2,4-difluorophenyl)ethynyl-cobalamin (3, F2PhEtyCbl)

Crystals of **3**, freshly grown from aqueous acetone (see above), were employed for diffraction experiments with a Nonius Kappa CCD diffractometer at a temperature of 233 K. Diffraction data extended to a resolution of 0.91 Å. The asymmetric unit of the orthorhombic crystal contained one B_{12} molecule and 11 water molecules with partial disordered positions.

Indexing of diffraction images, intensity integration, and data scaling were performed with programs DENZO and SCALEPACK.[3] The crystal was orthorhombic (space group $P2_12_12_1$) with unit cell constants a=15.9898(3) Å, b=21.5800(4) Å, and c=23.9084(5) Å. The structure was solved by direct methods and refined against F^2-values using the program SHELXL. [4] Full matrix least-squares anisotropic refinement converged at $R1$=0.0639 for all data. No absorption correction was applied to the data. The solvent region was modeled using 11 water molecules with anisotropic atomic displacement parameters (adp) at ordered and disordered molecules in major positions. H-Atom positions of **3** were calculated and refined as 'riding' on their respective non-H-atom. For methyl- and hydroxyl-groups the torsion angle around the C-C or C-O bond was also refined (omitted for water molecules). The isotropic adp for each H-atom was set to 1.5 times (for methyl- and hydroxyl-groups) and 1.2 times (for all other hydrogen atoms) the equivalent isotropic atomic displacement parameters of the adjacent non-H-atom. Data pertaining to diffraction data collection and structure refinement are summarized in Table S1.

The geometry of the inner coordination sphere of the cobalt is comparable to that of CNCbl or PhEtyCbl (**2**). Bond distances in the equatorial plane are (in Å) 1.877(5) (Co-N1), 1.908(4) (Co-N2), 1.911(4) (Co-N3) and 1.881(4) (Co-N4). The distances to the axial ligands are 1.877(7) Å (Co-C_β) and 2.071(5) Å (Co-N_α), the axial coordinative bonds C(1L)-Co-N(3N) are nearly linear (178.5(2)), the co-atom is displaced from the corrin plane by 0.005(2) Å towards N3N of the DMB base. The phenyl ring of the β-ligand is oriented North-South relative to the corrin ring (torsion angle C5-Co-C3L-C4L: 29.1°). The fold angle of the corrin ring is 18.6(1)°.

The supplementary crystallographic data of **3** were deposited as CCDC-1530214. Copies of the data can be obtained, free of charge, at the Cambridge Crystallographic Data Centre.

Table S1. Crystallographic data for F2PhEtyCbl (3)

Empirical formula	$C_{70}\ H_{91}\ Co\ F_2\ N_{13}\ O_{14}\ P$ x 11 H_2O	
Formula weight	1664.63	
Temperature	233(2) K	
Wavelength	0.71073 Å	
Crystal system	Orthorhombic	
Space group	$P2_12_12_1$ (no. 19)	
Unit cell dimensions	a = 15.9898(3) Å	α= 90°.
	b = 21.5800(4) Å	β= 90°.
	c = 23.9084(5) Å	γ = 90°.
Volume	8249.8(3) $Å^3$	
Z	4	
Density (calculated)	1.340 g/cm^3	
Absorption coefficient	0.314 mm^{-1}	
F(000)	3536	
Crystal size	0.250 x 0.080 x 0.060 mm^3	
θ_{max} for data collection	23.0° (0.91 Å resol.).	
Index ranges	-17<=h<=17, -23<=k<=23, -26<=l<=26	
Reflections collected	40613	
Independent reflections	11462 [R(int) = 0.0624]	
Completeness to theta = 22.99°	99.7 %	
Refinement method	Full-matrix least-squares on F^2	
Data / restraints / parameters	11462 / 0 / 1044	
Goodness-of-fit on F^2	1.060	
Final R indices [I>2sigma(I)]	R1 = 0.0507, wR2 = 0.1223	
R indices (all data)	R1 =0.0639, wR2 = 0.1293	
Absolute structure parameter	0.004(6)	
Largest diff. peak and hole	0.518 and -0.290 $e.Å^{-3}$	

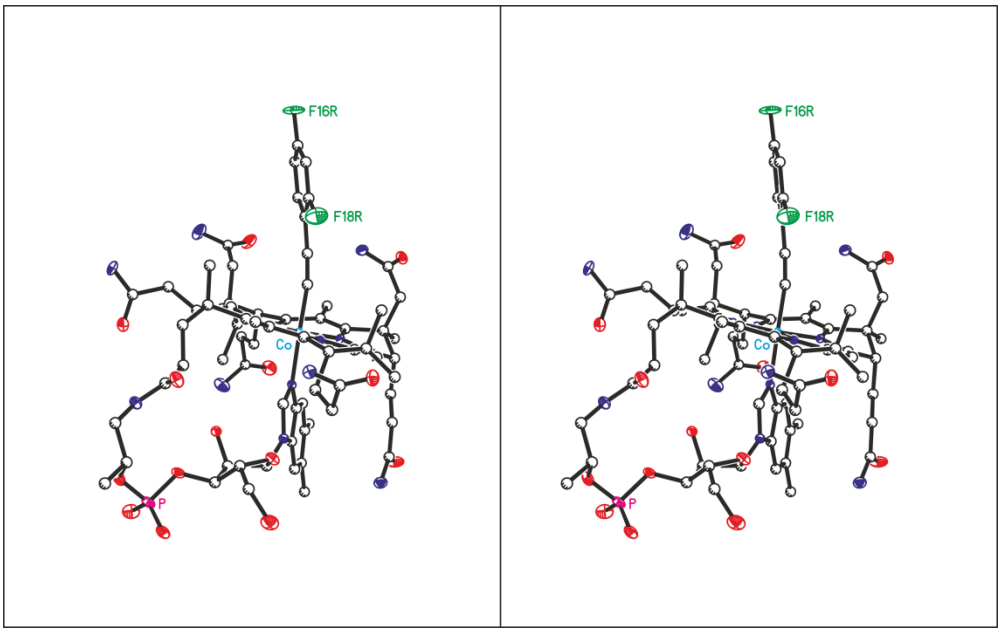

Figure S5. Stereo-model of the crystal structure of F2PhEtyCbl (**3**) with N, O, P Co and F atoms colored blue, red, orange, cyan and green, respectively.

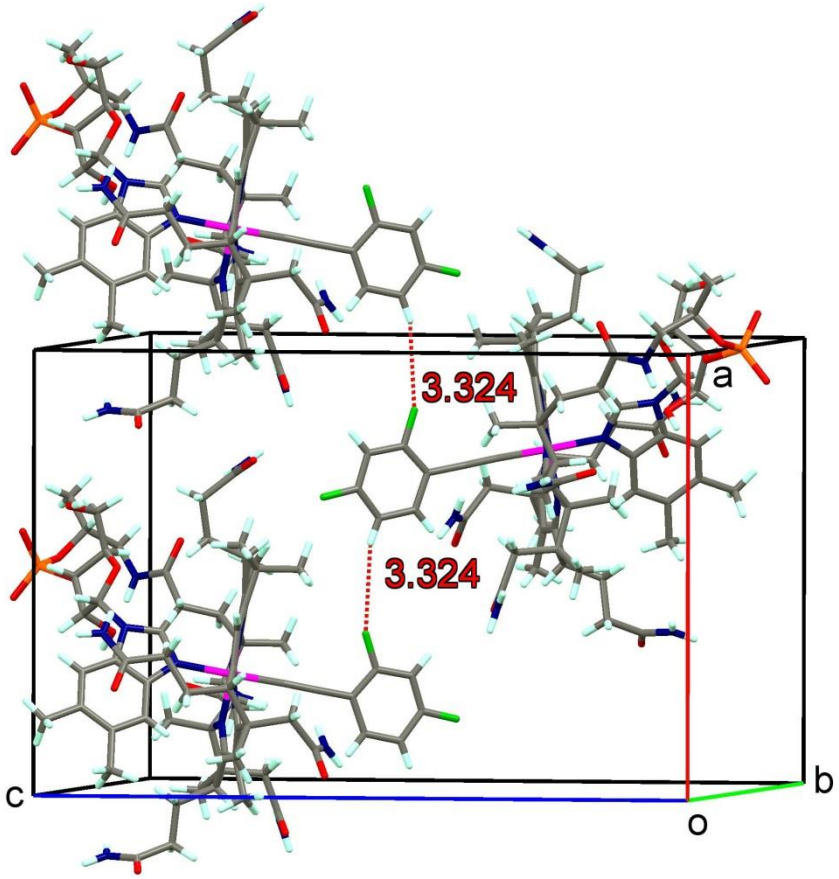

Figure S6. Crystal structure of F2PhEtyCbl (**3**) Elementary cell and selected intermolecular contacts between the F2PhEtyCbl molecules (with N, O, P Co and F atoms colored blue, red, orange, pink and green, respectively)**.**

Experiments testing the robustness of F2PhEtyCbl(3)

Thermolytic stability of F2PhEtyCbl (3):

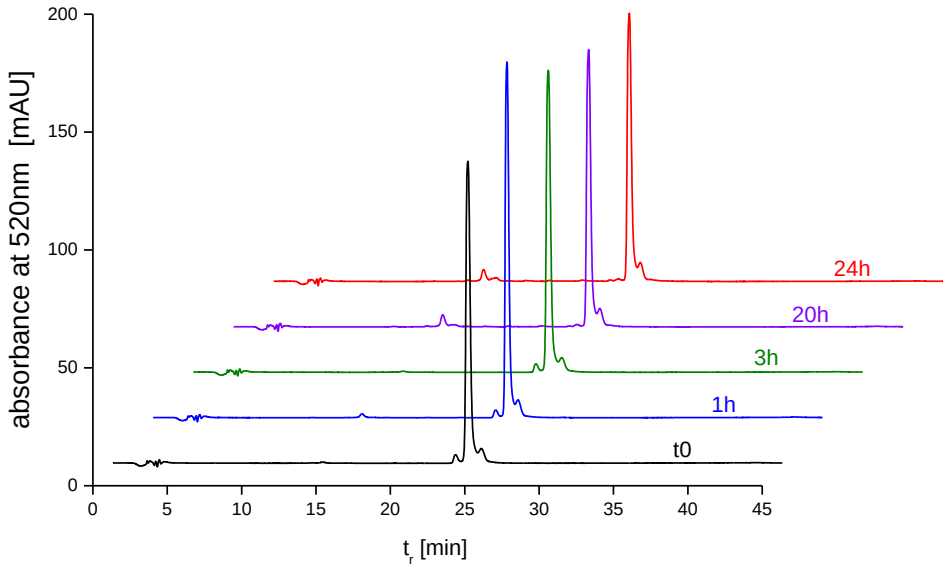

Figure S7: Thermolysis of F_2PhEtyCbl (**3**). HPLC analysis of solutions of **3** (c=7x10^{-4} M) in DMSO after thermolysis (protected from light) at 100°C under aerobic conditions for 0, 1h, 3h, 20h and 24h. (HPLC: Dionex Ultimate 3000; Phenomenex HyperClone ODS (C18) 120, 5 micron, 250x4.60mm; mobile phase A: 10mM potassium phosphate pH 7 B: MeOH, 8-95% in 40min, detection at 520 nm)

Test of light stability of 2-(2,4-difluorophenyl)ethynylcobalamin (3): In a UV/Vis cell a solution of F2PhEtyCbl(**3**) in H_2O (1×10^{-5} M) was exposed to daylight.

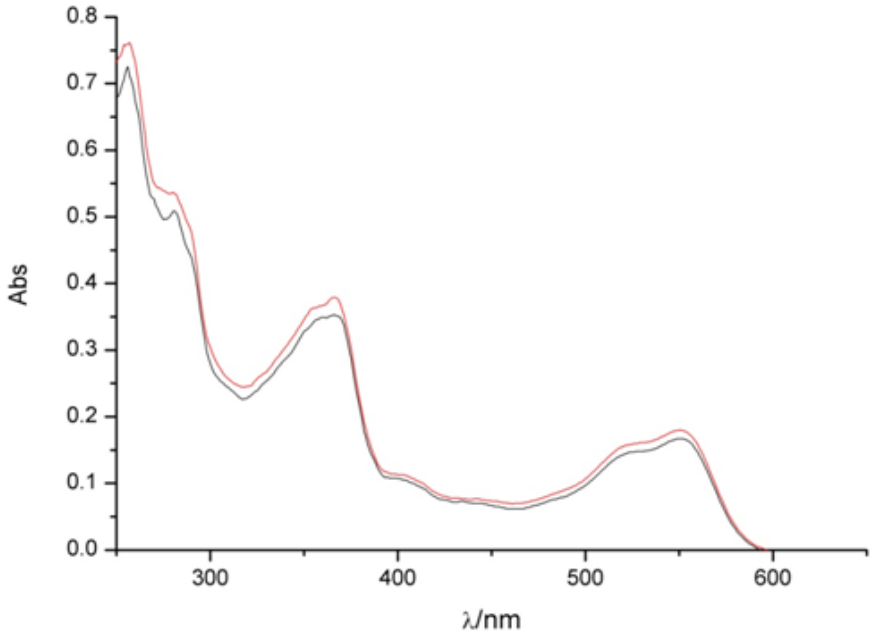

Figure S8. UV/Vis spectra of an aerated aqueous solution of F2PhEtyCbl (**3**), taken before (black line) or after 72 hours exposure to bright daylight (red line).

Hydrolytic decomposition of F2PhEtyCbl (3) at pH 2.
3 mg (2.05 µmol) of F2PhEtyCbl (**3**) were dissolved in 1 ml $H_2O_{dist.}$ and 50 µl of the resulting solution was diluted with 2.5 ml 100 mM phosphate buffer pH 2. The sample was stored under air at RT in the dark. UV/Vis spectra were recorded at regular intervals of time.

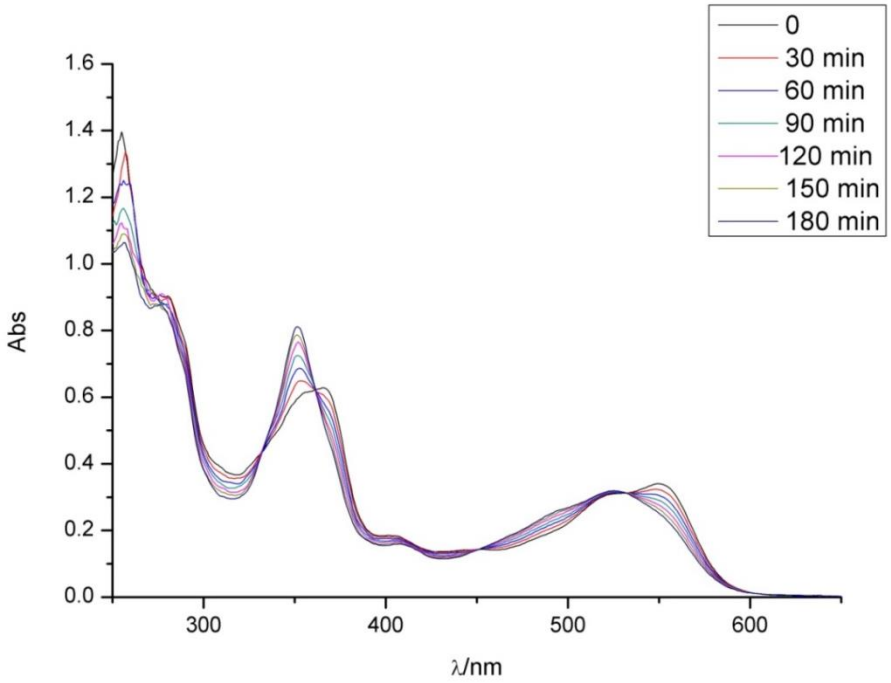

Figure S9: UV/Vis spectroscopic analysis of hydrolytic decomposition of an aerated aqueous solution of F2PhEtyCbl (**3**) in phosphate buffer pH 2 at room temperature.

Acid induced hydrolysis of F2PheEtyCbl (3) - pH-dependence of the rate.
Samples of 50 µl of a stock solution of F2PhEtyCbl (**3**) (1.0 µM) in water and 100 µl potassium phosphate buffers stock solution (100 mM, pH 2.0, 3.0 and 4.0) were diluted to 1.0 ml with water, respectively. For samples with < pH 2, 50µl of a stock solution with **3** were diluted with water and $HClO_4$ 70% was added to a final volume of 1.0 ml. UV/Vis spectra were recorded at regular time intervals. The changes in absorbance at 350 nm were plotted versus time and half-life ($\tau_{½}$) of hydrolysis was calculated using an exponential fit.

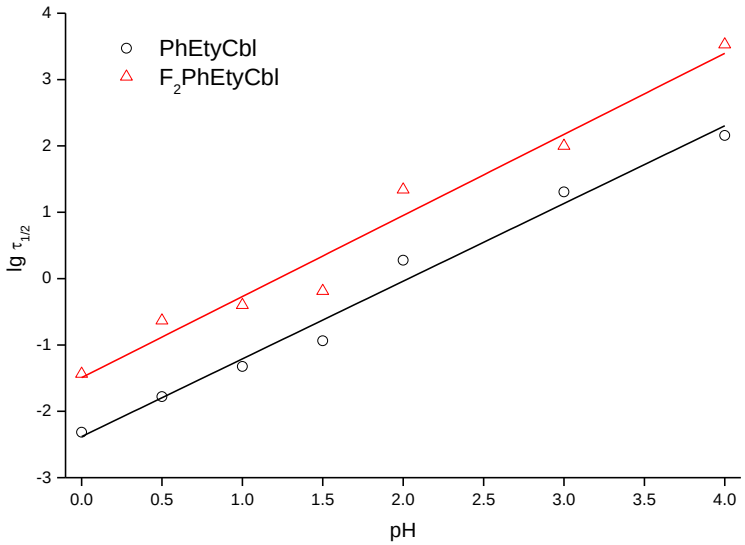

Figure S10: pH dependence of the half-life $\tau_{1/2}$ [h] for the acidic hydrolysis of F_2PhEtyCbl (**3**, red triangles) and PhEtyCbl (**2**, black circles) in aqueous solution ($c=5*10^{-5}$mol/l); pH values adjusted by $HClO_4$ (pH=0-1.5) and 10mM potassium phosphate buffer (pH≥2).

Determination of pKa of 3-H$^+$

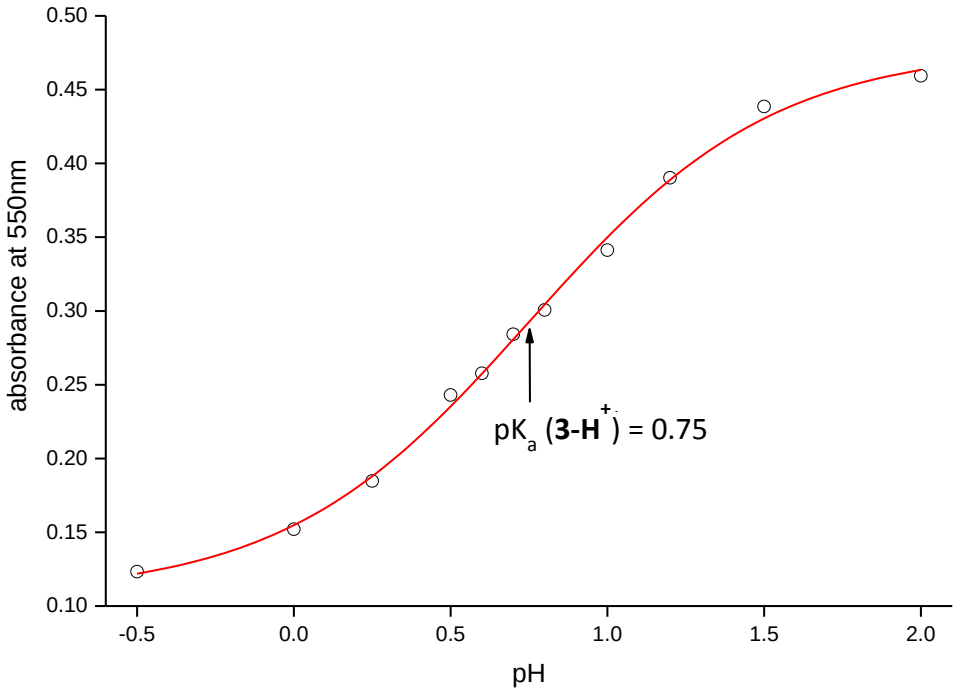

Figure S11. pH-Dependence of the equilibrium ('base-on') F2PhEtyCbl (**3**) vs. ('base-off') **3-H**$^+$ and determination of the pK$_a$ of **3-H**$^+$. Plot of absorbance at 550 nm (of F2PhEtyCbl, c=5.0x10^{-5} M) vs. pH (spectra were recorded within less than 10 sec after addition of acid).

Biochemical Experiments with human CblC

Binding of PhEtyCbl (2) and F2PhEtyCbl (3) to CblC and reaction with glutathione (GSH). All reactions were monitored at 20°C on a Varian Cary-100 spectrophotometer connected to a temperature-controlled water bath (600nm/min scan rate). CblC[7] (50 μM final concentration) in 100 mM HEPES (pH 7.4), 150 mM KCl, 10% glycerol buffer was added to a 200 μL cuvette containing 18-20 μM free either PhEtyCbl (**2**) or F2PhEtyCbl (**3**) and changes associated with binding were recorded. When no more changes in the UV-Vis spectra were observed, 10 mM glutathione (GSH) was added to the cuvette. Alternatively the enzyme was pre-incubated with GSH (10 mM) and Cbls were added to the CblC•GSH mixture.

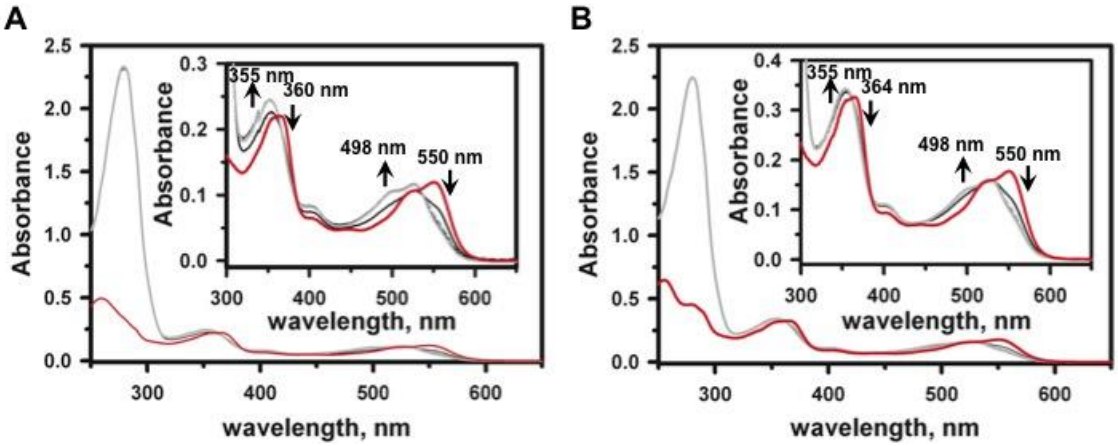

Figure S12. Binding of PhEtyCbl and F2PhEtyCbl to human CblC. Time-dependent spectral changes associated with binding of (A) PhEtyCbl (18 μM, red trace), or (B) F2PhEtyCbl (20 μM, red trace) to 50 μM CblC in 100 mM HEPES buffer, pH 7.4 containing 150 mM KCl and 10 % glycerol. Spectra were recorded every minute between 1 and 60 min at 20 °C and a subset is shown for clarity: t = 1 min (red trace), 20 min (black trace) and 60 min (grey trace) A blue shift in the spectra was observed for the CblC-bound PhEtyCbl and F2PhEtyCbl derivatives (gray traces A,B).

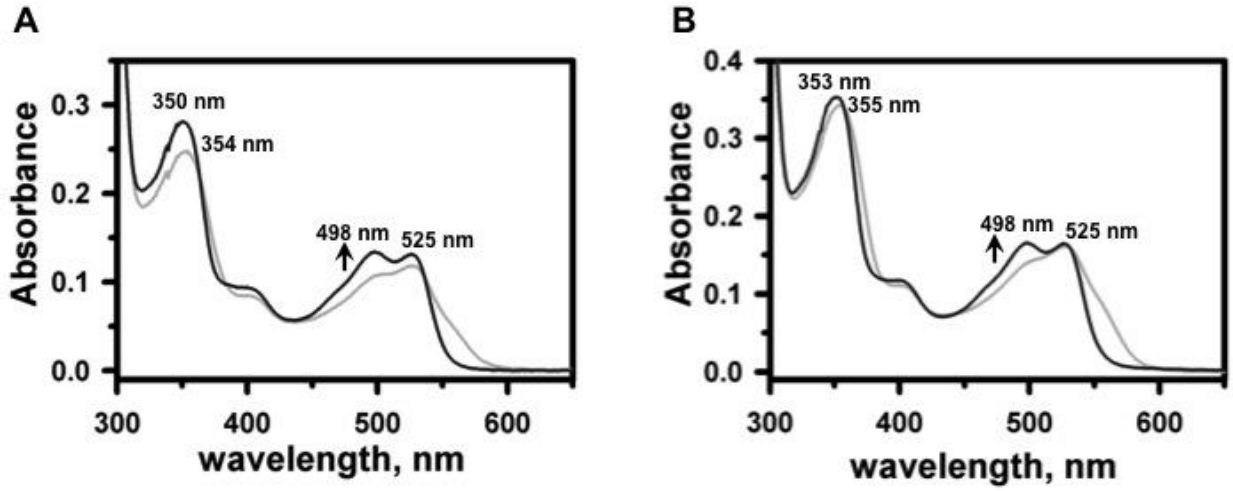

Figure S13. Effect of GSH on CblC•PhEtyCbl (**2**) (A) and CblC• F2PhEtyCbl (**3**) (B). Spectroscopic changes associated with the interaction between 10 mM GSH and CblC• PhEtyCbl (50:20 μM) and CblC•F2PhEtyCbl (50:20 μM) in 100 mM HEPES (pH 7.4), 150 mM KCl, 10% glycerol containing buffer were monitored at 20°C during a time of 12 hours . The reaction was initiated by addition of GSH to holo-CblC (grey trace) and an immediate hypsochromic shift in the spectra was observed (black trace). No additional changes were observed up to 12 h.

HPLC analysis of Cbl products from incubation of CblC•PhEtyCbl (50:20 μM) or CblC•F2PhEtyCbl (50:20 μM) with 10 mM GSH at 20C for 1-12 hours. Cbls were detected by HPLC following quenching by heat inactivation at 70°C for 20 min and centrifugation to remove the precipitate. Cbls were analyzed by gradient reverse-phase HPLC using an Agilent 1100 System equipped with a Phenomenex C-18 column (250×4.6 mm, 5 μM particle size). Solvent A: 0.1% acetic acid /acetate buffer pH 3.5 (adjusted with NH_4OH), solvent B: MeCN containing 0.1% acetic acid. Solvent composition: 0 – 2 min: 0 – 5% B, 2-14min: 5 – 15% B, 14-19 min: 15-18% B; 19 – 32 min: 18 – 35% B, 32 – 33 min: 35 – 60 % B, 32 – 35 min: 60 – 5% B

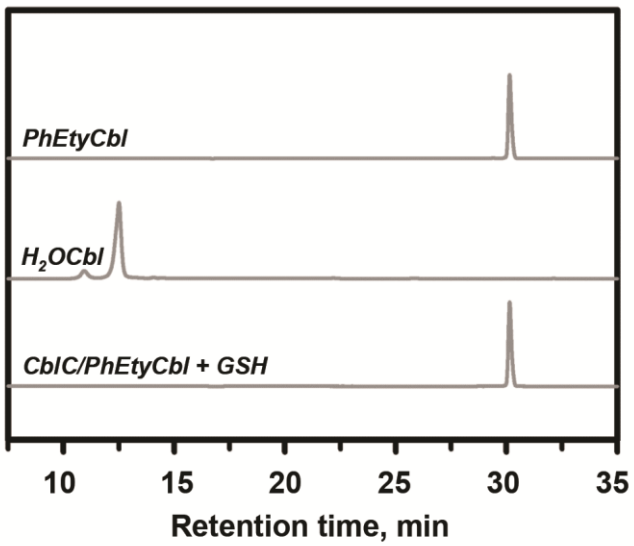

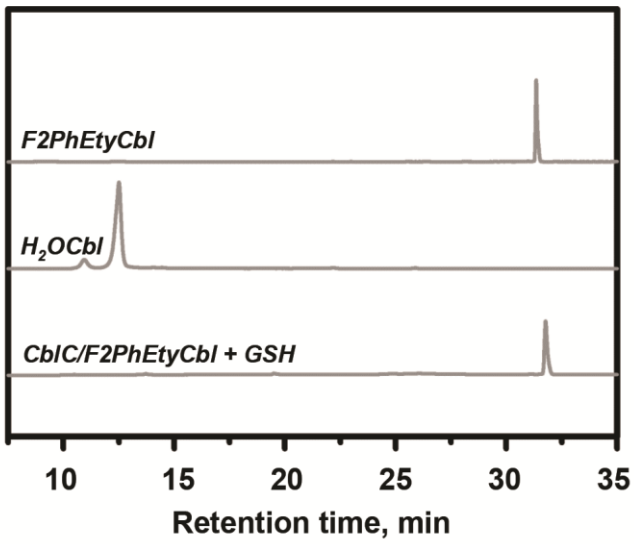

Figure S14. HPLC analysis of Cbl derivatives recovered after incubation with CblC and GSH, described as CblC● PhEtyCbl (top) and CblC●F2PhEtyCbl (bottom). Reaction mixtures containing 17-20 μM Cbl derivatives and 50 μM CblC in 100 mM HEPES (pH 7.4), 150 mM KCl, 10 % glycerol buffer were incubated with 10 mM GSH for 12 hours at 20°C. The Cbls of the reaction products at 12 hours were released from the enzyme and recovered for HPLC analysis, as described above). The HPLC-elution profiles of the reaction mixtures (shown as lower traces), as well as of H_2OCbl, PhEtyCbl and F2PhEtyCbl standards (shown in the upper two traces, resp.) in the two panels were detected at 350 nm.

Binding of PhEtyCbl (2) and F2PhEtyCbl (3) to CblC *monitored by isothermal titration calorimetry (ITC)* – ITC experiments were performed using a Microcal VP-ITC (GE Healthcare). All experiments were performed at 20°C in 100 mM HEPES (pH 7.4), 150 mM KCl, 10% glycerol buffer. The enzyme (10-12μM of CblC alone or in the presence of 1mM GSH) was titrated with 37 aliquots (8 μL) of a 200-220 μM solutions of PhEtyCbl and F2PhEtyCbl (in the presence or absence of 1mM GSH). The calorimetric signals were integrated and data was analyzed with Microcal ORIGIN software using a single-site-binding model to determine the equilibrium association constant, $K_A = (1/K_d)$ and the binding enthalpy, $\Delta H°$. All binding curves had *N*-values between 0.9-1.0.

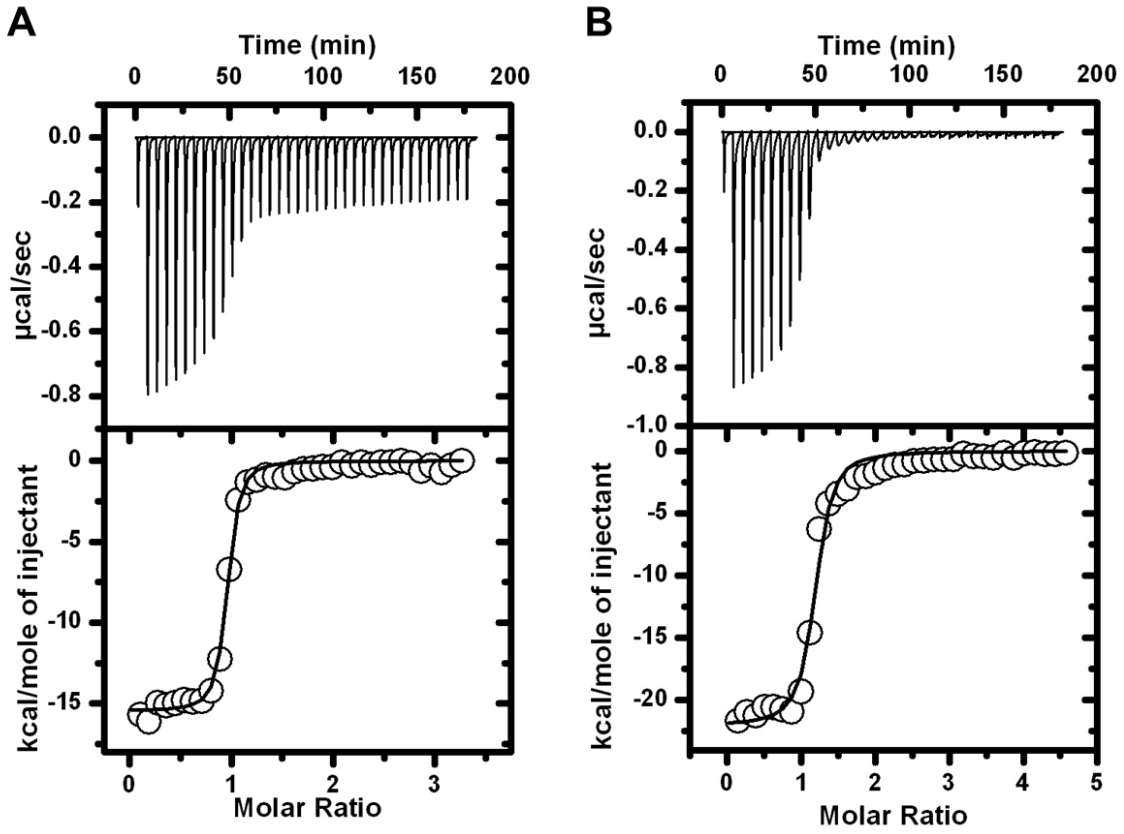

Figure S15. Isothermal titration calorimetry (ITC) analysis of PhEtyCbl (**2**) and F2PhEtyCbl (**3**) binding to CblC. Calorimetric data for a representative titration of 10 μM CblC (in the presence of 1mM GSH) with 200 μM PhEtyCbl (**2**) (in the presence of 1mM GSH) (A) and 200 μM F2PhEtyCbl (**3**) (in the presence of 1 mM GSH). The binding isotherm (lower panel) was fitted to a one-binding site model.

Table S2. Dissociation constants and binding enthalpies of phenylethynylcobalamin (PhEtyCbl, **2**) and of 2,4-difluorophenylethynylcobalamin (F2PhEtyCbl, **3**) to CblC in the presence of 1mM GSH

Cbl-ligand	K_D *(nM)*	**Δ*H* *(kcal/mol)***
PhEtyCbl (2)	30 ± 5.6	-15 ± 0.17
F2PhEtyCbl (3)	129.5 ± 13.0	-22 ± 0.42

Protein Crystallography

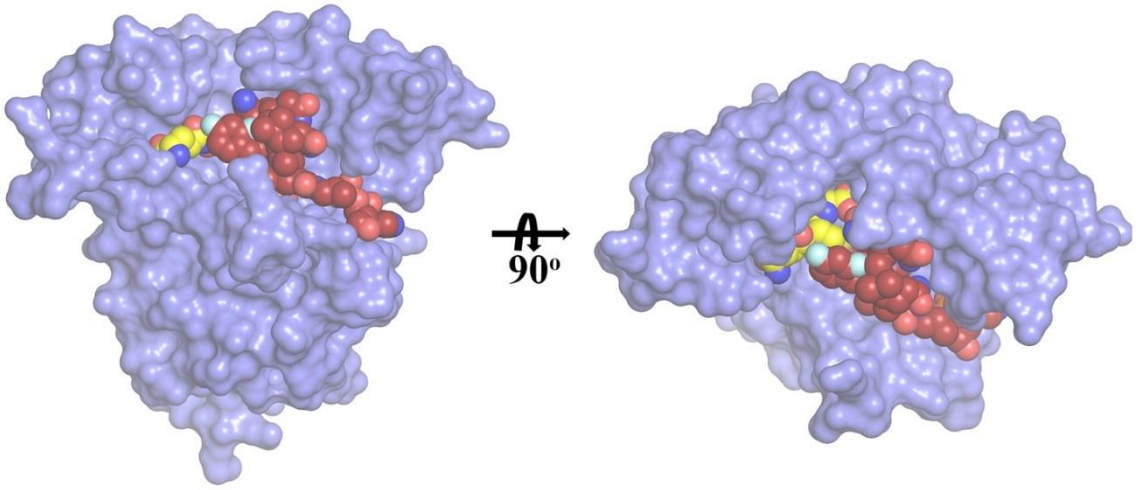

Figure S16. Surface representation of GSH and F2PhEtyCbl (**3**) bound CblC (blue) in two different oritentations. GSH and F2PhEtyCbl are shown in yellow and dark red spheres respectively.

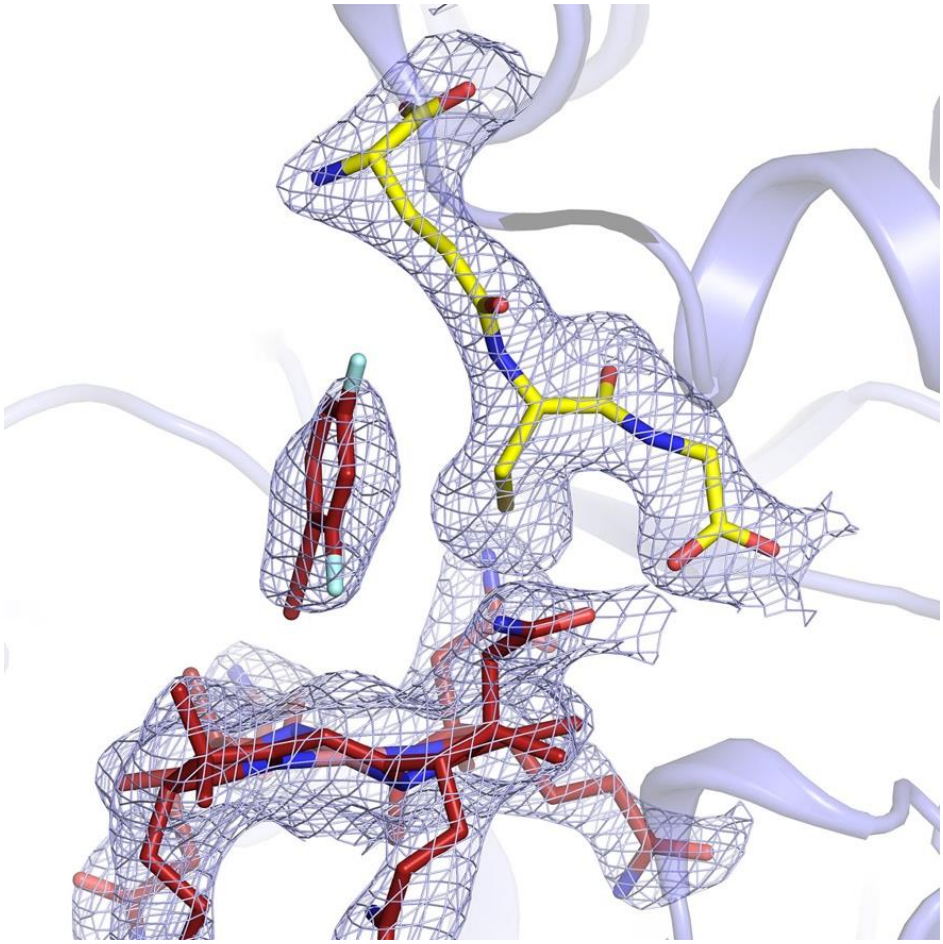

Figure S17. Electron density corresponding to the **GSH** and **F2PhEtyCbl** ligands bound to CblC. The refined composite omit 2Fo-Fc difference density map for GSH and F2PhEtyCbl contoured at 1.5σ is shown in light blue. GSH and F2PhEtyCbl are shown in yellow and dark red sticks.

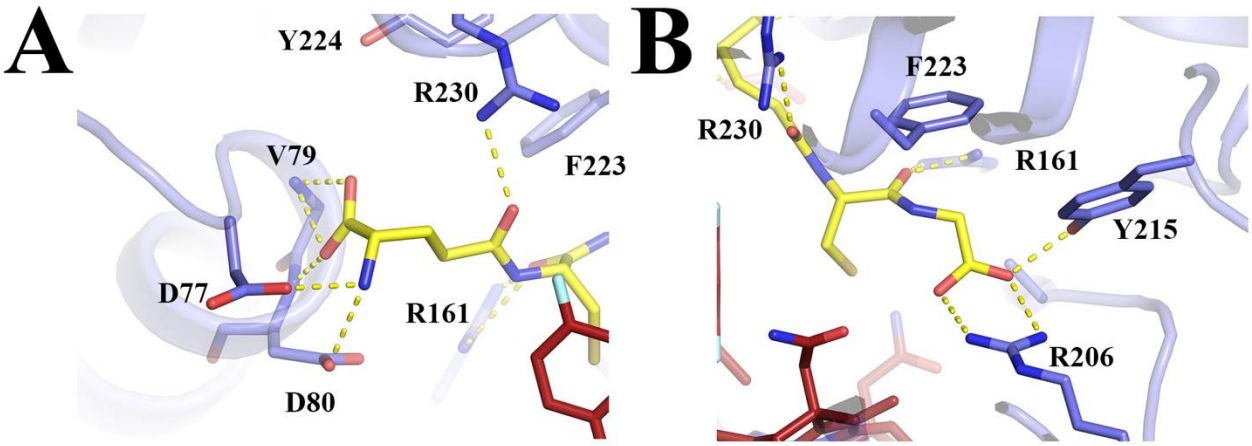

Figure S18. GSH binding environment in the ternary complex with CblC and the Cbl **3**. **A** Close-up of the glutamate moiety and **B** close up of the glycine moiety of the GSH tripeptide. Cartoon and color representation are as described for **Figure 6A**.

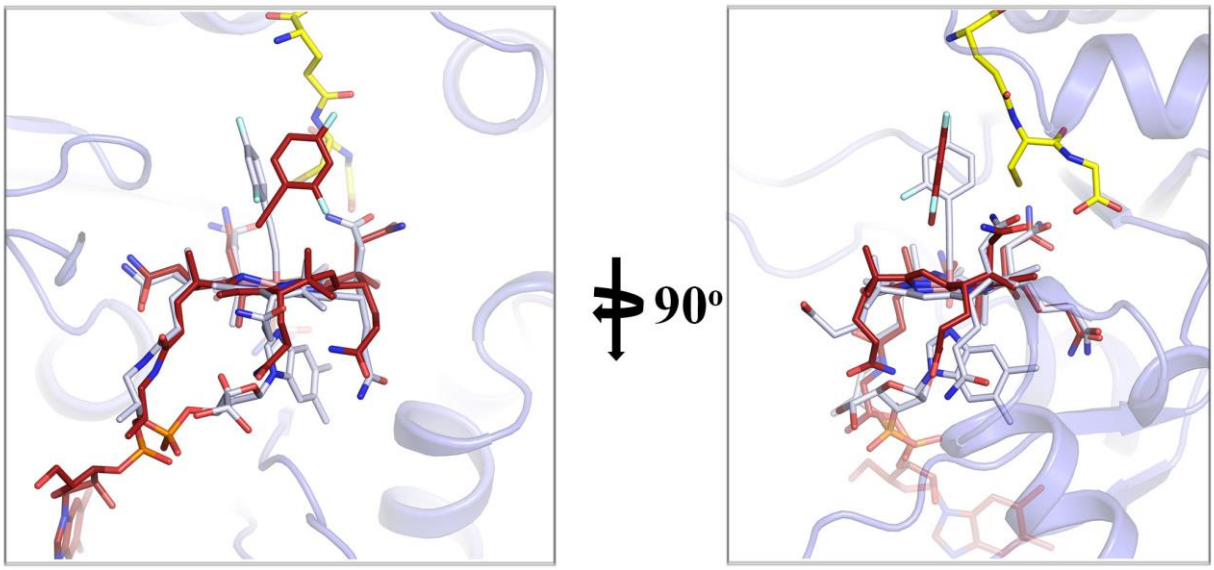

Figure S19. Two views of the structural superposition of free F2PhEtyCbl **3** (gray) with the crystallographically investigated ternary complex of CblC (light blue) with GSH (yellow) and **3** (dark red).

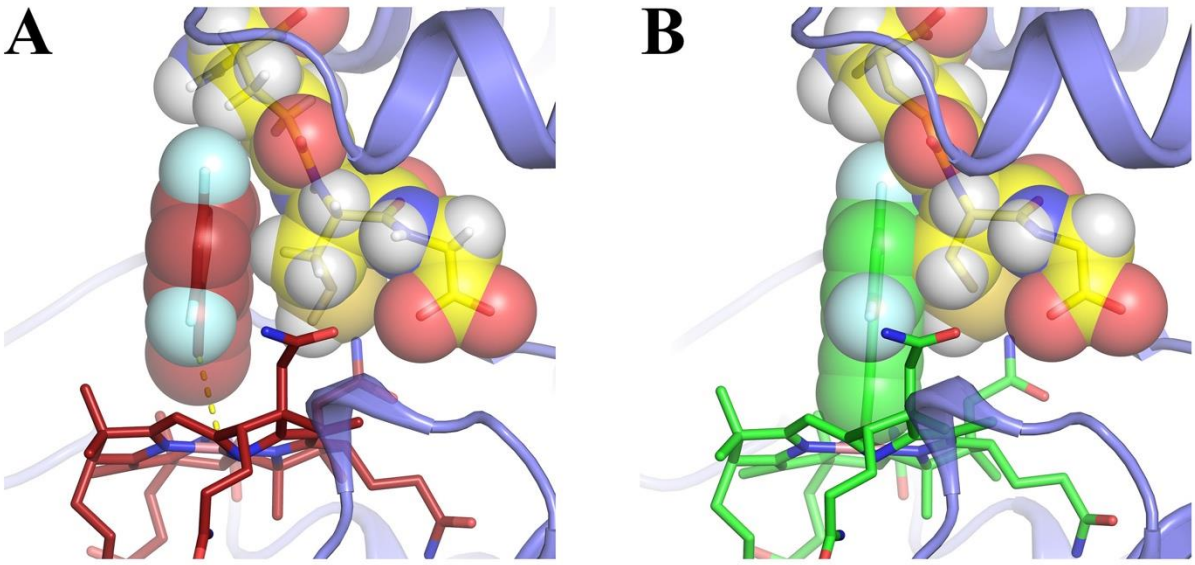

Figure S20. A. Close in the active site demonstrating the tight packing of the GSH (yellow) and the F2PhEty ligand (dark red) shown in van der Waal's spheres. Cbl-moiety is also shown in dark red. **B** Model of the F2PhEty ligand (green speheres) of intact F2PhEtyCbl (**3**, green sticks), however with the aromatic ring of the F2PhEty ligand in the same orientation as in **A**. Steric clashes with GSH (yellow spheres) are evident.

Table S3. Protein Crystallographic data. Data processing and refinement statistics.

Protein	**CblC + F2PhEtyCbl + GSH**
Data Collection	
Space Group	$P6_122$
Cell Dimensions	
a, b, c (Å)	114.5, 114.5, 151.0
α, β, γ (°)	90, 90, 120
Wavelength (Å)	1.033
Resolution (Å)	50-2.51 (2.62-2.51)
R_{sym} (%)	9.1 (66.8)
I/σI	21.2 (3.8)
CC(1/2)	0.999 (0.853)
Completeness (%)	86.3 (87.8)
Redundancy	12.3 (11.7)
Refinement	
Resolution (Å)	99.1-2.51
No. reflections	16,527
R_{work} / R_{free}	0.176 / 0.214
No. atoms	
Protein	1928
Water	75
B12	91
GSH	20
8FS	10
B-factors	
Protein	51.7
Water	47.6
B12	48.1
GSH	52.7
8FS	72.6
R.m.s Deviations	
Bond lengths (Å)	0.013
Bond angles (°)	1.178
Ramachandran plot (%)	
Favored/allowed/outliers	97.05/2.95/0
MolProbity Score	1.32 (100^{th} percentile)
Protein Data Bank code	**5UOS**

Crystallization of CblC ternary abortive complex CblC-4. For crystallization purposes, His tag cleaved human CblC (CblC) was run through size exclusion column (S200; GE Healthcare) and eluted in 50 mM tris-pH 8.0 and 0.5mM TCEP. CblC was then reconstituted with 250μM F2PhEtyCbl (**3**) and 1mM GSH. The resulting protein sample was then concentrated to 12 mg ml^{-1} in 50 mM tris-pH 8.0 and 0.5mM TCEP and after passing through a Spin-X centrifuge filter (Corning Costar) was used for crystallization screening. Crystals of the ternary complex **CblC-4** (of **3**, GSH and CblC) were grown by the sitting drop vapor diffusion method at 4 ºC by mixing 2 μl of protein solution with 1 μl of reservoir solution, which contained 0.2 M NaCl, 0.1 M CHES:NaOH at pH 9.5 and 1.26 M ammonium sulfate. Crystals were cryoprotected for a few minutes before being flash frozen in liquid N_2, by transfer to a solution of 15 % glycerol, 0.15 mM NaCl, 0.075 mM CHES:NaOH at pH 9.5, and 1 M ammonium sulfate. Crystals of **CblC-4** were of space group $P6_122$ (a= b= 114.5 Å, c= 151.0 Å, α= β= 90°, γ= 120°) with 1 monomer in the asymmetric unit (Matthews' coefficient, V_M = 5.25 $Å^3$/Da for 1 **CblC-4** monomer, 76.6% solvent content).

Data collection, structure determination and refinement. Diffraction data were collected at GM/CA-CAT 23-IDB (Advanced Photon Source, Argonne National Laboratory) on a Mar 300 detector and processed with HKL2000 [3] to 2.5 Å resolution. Initial phases were obtained by the molecular replacement (MR) method with Phaser [6] using a previous CblC structure[7] as a model (PDB accession number 3SC0). It has to be noted that all loops and areas with high B-factors as well as the MeCbl cofactor were omitted from the search model. Phaser successfully obtained a solution with a single monomer in the asymmetric unit. The **CblC-4** structure was refined originally with PHENIX [8] including simulated annealing in torsional and Cartesian space, coordination minimization, and restrained individual B-factor adjustment with maximum-likelihood targets. Refmac5 [9] in the CCP4i suite [10] was subsequently employed for restrained refinement of using isotropic individual B-factors with maximum-likelihood targets using the babinet model for bulk solvent scaling, followed by model building and modification with Coot [11]. Several iterative rounds of refinement followed by model building/modifications were performed. In the early rounds of refinement, no ligands were fitted. First, the cobalamin ligand without an axial ligand was fitted. Subsequently, very clear electron was assigned to GSH. GSH was fitted and refined against this density. Lastly 2,4-difluorophenyl-ethynyl (**F2PhEty)** ligand was originally fitted and refined against the electron density corresponding to the axial position above the Co atom. However, the electron density at this resolution was consistent with an aromatic ring that needed to be positioned further away from the Co atom. Moreover, based on the **F2PhEtyCbl** (**3**) free ligand crystal structure we expected the aromatic plane to almost coincide and being at a very narrow angle with respect to the axis of the Co atom. The electron density in our structure clearly indicated an aromatic ring that its plane laid parallel to the Co dz^2 orbital axis and translated away by at least 1 Å. Therefore, we posit that **3** has been photo-cleaved to a Co(II) species and a free ligand in the proximity of the Co atom, which was thus modeled and refined as **F2PhEty** (**8FS**). The ligand restraints for 2,4-difluorophenyl-ethynyl (**8FS**) in a .cif format that were required for refinement with Refmac5 were prepared via the PRODRG server [12]. The final model was used to create an unbiased refined composite 2Fo-Fc omit map with PHENIX. Crystallographic information as well as refinement statistics are provided in the (SuppInfo, Table S3. The geometric quality of the model and its agreement with the structure factors were assessed with MolProbity. For PRORP2, MolProbity [13] reported a clash and a molprobity score of 2.94 (100^{th} perecentile) and 1.19 (100^{th} percentile) respectively, while 97.5 % of the residues were in the favored Ramachandran plot regions with 0 % residues in outlier regions. Figures showing **CblC-4** crystal structures were generated with PyMOL[14].

References

[1] J. E. Hein, J. C. Tripp, L. B. Krasnova, K. B. Sharpless, V. V. Fokin, *Angew. Chem. Int. Ed.* **2009**, *48*, 8018-8021.

[2] M. Ruetz, R. Salchner, K. Wurst, S. Fedosov, B. Kräutler, *Angew. Chem. Int. Ed.* **2013**, *52*, 11406-11409.

[3] Z. Otwinowski, W. Minor, *Methods in Enzymology, Macromolecular Crystallography, Pt A* **1997**, *276*, 307-326.

[4] G. M. Sheldrick, *Bruker Analytical X-ray Instruments Inc. Madison, USA* **2014**.

[5] L. Hannibal, A. Axhemi, A. V. Glushchenko, E. S. Moreira, N. E. Brasch, D. W. Jacobsen, *Clinical Chemistry and Laboratory Medicine* **2008**, *46*, 1739-1746.

[6] A. J. McCoy, R. W. Grosse-Kunstleve, P. D. Adams, M. D. Winn, L. C. Storoni, R. J. Read, *Journal of Applied Crystallography* **2007**, *40*, 658-674.

[7] M. Koutmos, C. Gherasim, J. L. Smith, R. Banerjee, *J Biol Chem* **2011**, *286*, 29780-29787.

[8] P. D. Adams, R. W. Grosse-Kunstleve, L. W. Hung, T. R. Ioerger, A. J. McCoy, N. W. Moriarty, R. J. Read, J. C. Sacchettini, N. K. Sauter, T. C. Terwilliger, *Acta Crystallogr D Biol Crystallogr* **2002**, *58*, 1948-1954.

[9] G. N. Murshudov, P. Skubak, A. A. Lebedev, N. S. Pannu, R. A. Steiner, R. A. Nicholls, M. D. Winn, F. Long, A. A. Vagin, *Acta Crystallogr D Biol Crystallogr* **2011**, *67*, 355-367.

[10] E. Potterton, P. Briggs, M. Turkenburg, E. Dodson, *Acta Crystallogr D Biol Crystallogr* **2003**, *59*, 1131-1137.

[11] P. Emsley, B. Lohkamp, W. G. Scott, K. Cowtan, *Acta Crystallogr D Biol Crystallogr* **2010**, *66*, 486-501.

[12] A.W. Schüttelkopf and D.M.F. van Aalten. *Acta Crystallogr.* 2004, D60, 1355–1363.

[13] I. W. Davis, A. Leaver-Fay, V. B. Chen, J. N. Block, G. J. Kapral, X. Wang, L. W. Murray, W. B. Arendall, 3rd, J. Snoeyink, J. S. Richardson, D. C. Richardson, *Nucleic Acids Res* **2007**, *35*, W375-383.

[14] Schrodinger, LLC, **2010**.